Environmental Science Nano

Humic acid mitigated toxicity of graphene-family materials to algae through reducing oxidative stress and heteroaggregation

Journal:	*Environmental Science: Nano*
Manuscript ID	EN-ART-01-2019-000067.R1
Article Type:	Paper
Date Submitted by the Author:	14-Apr-2019
Complete List of Authors:	Zhao, Jian; Ocean University of China Li, Yue; Ocean University of China Cao, Xuesong; Ocean University of China Guo, Chuntong; Ocean University of China Xu, Lina; Ocean University of China, College of Environmental Science and Engineering Wang, Zhenyu; Jiangnan University, Feng, Juan; Qingdao University Yi, Huimin; Ocean University of China Xing, Baoshan; UMASS, Stockbridge School of Agriculture

Environmental Significance

Adverse effect of graphene-family materials (GFMs) on aquatic organisms has attracted increasing attention. However, natural organic matter may alter GFMs-induced toxicity. Our work demonstrated that GFMs-induced toxicity to algae was highly mitigated by humic acid (HA), and the antagonistic degree followed the order of rGO>GO>G. The alleviation in membrane damage by HA was a main mechanism for the observed toxicity mitigation, through decreasing both oxidative stress and GFMs-algae direct contact. The direct contact was lowered by weakened GFMs-algae heteroaggregation (for rGO and G) and enhanced steric hindrance (for GO, rGO and G). The findings will be helpful for better understanding the environmental risk of different GFMs in natural aquatic environments.

Humic acid mitigated toxicity of graphene-family materials to algae through reducing oxidative stress and heteroaggregation

Jian Zhao,[a,b] Yue Li,[a] Xuesong Cao,[a] Chuntong Guo,[a] Lina Xu,[a] Zhenyu Wang,[b,c] Juan Feng,[d] Huimin Yi,[a] and Baoshan Xing*[,e]

[a] Institute of Coastal Environmental Pollution Control, and Ministry of Education Key Laboratory of Marine Environment and Ecology, Ocean University of China, Qingdao 266100, China

[b] Laboratory for Marine Ecology and Environmental Science, Qingdao National Laboratory for Marine Science and Technology, Qingdao 266071, China

[c] Institute of Environmental Processes and Pollution Control, and School of Environmental and Civil Engineering, Jiangnan University, Wuxi 214122, China

[d] College of Environmental Science and Engineering, Qingdao University, Qingdao 266071, China

[e] Stockbridge School of Agriculture, University of Massachusetts, Amherst, Massachusetts 01003, United States

*Corresponding author

Tel.: +1 413 545 5212; fax: +1 413 577 0242

E-mail address: bx@umass.edu (Dr. Baoshan Xing)

Abstract

Graphene-family materials (GFMs) will be released into natural aquatic environments during their increasing applications, thus likely inducing adverse effects on aquatic organisms. This work systematically investigated the effect of natural organic matter on the toxicity of GFMs to algae *(Chlorella pyrenoidosa)*. Toxicity antagonism was observed between humic acid (HA) and all the three types of GFMs, and the degree of antagonism in the presence of HA followed the order: reduced graphene oxide (rGO) > graphene oxide (GO) > graphene (G). rGO showed the highest mitigation in membrane damage (29.3%) by HA in comparison with GO (22.9%) and G (28.4%), demonstrating that the reduction in membrane damage was a main mechanism for toxicity mitigation by HA. HA could alleviate GFMs-induced membrane damage through decreasing oxidative stress as confirmed by lower intracellular reactive oxygen radicals (ROS) and malondialdehyde content in the presence of HA. The decrease in direct contact between GFMs and algae was another reason for the membrane damage mitigation, and the direct contact was lowered by weakened GFMs-algae heteroaggregation (for rGO and G) and enhanced steric hindrance (for GO, rGO and G). In addition, for GO, the nutrient depletion correction (e.g., Mg) was also responsible for the toxicity mitigation by HA, while HA did not correct nutrient depletion that induced by rGO and G. These findings suggest that natural organic matter is of importance for better understanding the environmental risk of GFMs in aquatic environments.

Keywords: Joint toxicity; Natural organic matter; Membrane damage; Heteroaggregation; Adsorption; Nutrient depletion

1 Introduction

Graphene-family materials (GFMs) include graphene (G) and graphene derivatives, such as graphene oxide (GO) and reduced graphene oxide (rGO).[1] The extraordinary optical, electrical and medical properties of GFMs have attracted industrial, commercial and scientific extensive attentions.[2,3] With increasing production and application, GFMs will be discharged into aquatic environments,[4] and the concerns on the potential negative impact on aquatic organisms are rapidly increasing.

It was reported that GFMs exhibited significant toxicity to aquatic organisms such as bacteria,[5-7] algae,[8,9] crustaceans,[10] nematodes,[11] and fish.[12] The main toxicity mechanisms include physical penetration into cell wall/membrane by direct contact, oxidative stress and lipid peroxidation, charge transfer between biological membrane and GFMs, as well as accumulation in cells/organs of organisms.[6-12] For example, GO exhibited strong shading effect on algal growth and induced membrane damage mainly through oxidative stress, while rGO and G tended to heteroaggregate with algae and extracted phospholipid from the cell membrane when directly contacting with algal cells.[8] Chen et al. also reported that the interaction pattern between GO and bilayer, which differed from G.[13] It can be concluded that different types of GFMs had different toxicity mechanisms to aquatic organisms. In addition, it is circumscribed to only investigate toxicity of GFMs under laboratory conditions without considering natural environmental factors such as natural organic matter (NOM).[14] NOM exists abundantly in the aquatic environment and has the potential to affect the toxicity of GFMs to aquatic organisms.

It is well known that NOM could be adsorbed on the surface of carbon nanomaterials, and

alter their dispersion/aggregation behaviors. The related surface modification and dispersion alteration of carbon nanomaterials can change the physical contact with aquatic organisms, which is recognized as an important mechanism for the toxicity from carbon nanomaterials such as GFMs.[1] This physical contact is particularly important for unicellular organisms such as bacteria and algae because these unicellular organisms could be sufficiently attached by GFMs through the formation of heteroaggregates.[15] Meanwhile, the change in dispersion/aggregation of GFMs may lower the light availability of primary producers such as algae, thus inducing indirect toxicity. Therefore, algae should be a sensitive and typical species for identifying the role of NOM in GFMs-induced toxicity. For algae, there are two studies to report that NOM reduced GFMs-induced toxicity to green algae *Scenedesmus obliquus*.[16,17] Specially, Zhang et al. did a mechanistic investigation, and found that the reductions in growth and Chlorophyll-a (Chl-a) synthesis were related to decreased GFM-algae contact and intracellular reactive oxygen species (ROS) generation in *Scenedesmus*.[17] However, shading effect and nutrient depletion from GFMs (especially for GO) are important reasons for the inhibition of algae growth and Chl-a synthesis,[8] which should be further considered when investigating the toxicity of GFMs in the presence of NOM. The heteroaggregation between GFMs and algae could be a crucial process to explain physical contact and membrane damage, but the effect of NOM on GFM-algae heteroaggregation was not investigated in previously published works. Actually, the algae *Scenedesmus* species are mainly in the form of their colonies in medium and natural waters,[18,19] which is not an excellent model algal species for the investigations on GFM-algae

heteroaggregation and related membrane damage. Previous works reported much higher sensitivity of *Chlorella* than *Scenedesmus* to various nanoparticles (NPs) (e.g., TiO_2, ZnO, Ag) due to the single-cell individual, thinner pectic layer and less-resistant cell wall, and specific defense mechanism of *Chlorella*.[18,19,20] Therefore, *Chlorella* was chosen as a model algal species to further examine the toxicity of GFMs in the presence of NOM. In addition, Lu et al. found that humic acid (HA) enhanced the accumulation of G (O content < 10%) in zebrafish by a factor of 2.5-16 times.[21] On the contrary, HA lowered the bioaccumulation of GO, which had higher O content, in the body of *Daphnia magna*.[16] It seems that the toxicity alteration by HA highly related to the surface functional groups of GFMs. The interaction (e.g., adsorption, dispersion stability) of NOM with carbon nanomaterials such as GFMs and carbon nanotubes (CNTs) depends on the contents of O-containing groups of these carbon nanomaterials.[22,23] Therefore, the alteration mechanism by NOM may be different among the GFMs with different oxidation degrees, which will be investigated in the present work.

Therefore, three typical and frequently-used GFMs (GO, rGO, and G) have been chosen to explore the effect of NOM on GFMs-induced toxicity to common freshwater algae *Chlorella pyrenoidosa* (*Chlorella sp.*). The objectives were to (1) investigate the influence of NOM on the toxicity of the three GFM types to algae; (2) explore the alteration mechanisms of GFM toxicity caused by NOM; and (3) identify the role of GFM properties (e.g., functional group content) in the observed toxicity alteration. This work will provide information for more accurately evaluating the risks of GFMs in natural aquatic environments.

2. Materials and methods

2.1 Material characterization

GO was prepared by the modified Hummers' method.[24] Briefly, graphite (3.0 g) was added into a flask with H_2SO_4/H_3PO_4 (270 mL/30 mL) and stirred in ice-bath, then 18 g $KMnO_4$ was added into the flask slowly. The mixture was stirred in 50 °C water bath for 15 h. Then, 30% H_2O_2 (10 mL) was added slowly until the mixture was transformed to luminous yellow suspension (around 20 min). Then, the suspension was sonicated for 30 min, and washed under centrifugation with hydrochloric acid (10%) (6000 rpm, 10 min), ethyl alcohol (8600 rpm, 10 min), and ultrapure water (18000 rpm, 30 min), respectively. Finally, the pH of suspension reached 5.0, and GO was obtained by freeze drying. rGO and G were purchased from Graphene Supermarket (USA). HA and citric acid (CA) were purchased from Sigma-Aldrich (USA), and Sinopharm Chemical Reagent Co. (China), respectively.

Morphology of GFMs (GO, rGO, and G) was characterized using transmission electron microscopy (TEM, Hitachi, H-7650, Japan). Elemental compositions of the three GFMs and HA were determined by elemental analyzer (Vario MicroCube, Elementar, Germany). The structural properties of GFMs were analyzed by Raman spectroscopy (Thermo Fisher, USA), and the sp^2/sp^3 carbon atom ratio was shown by *D*/*G* peak intensity (I_D/I_G). The hydrodynamic diameter and zeta potential of GFMs in ultrapure water (pH, 7.0) were measured by Zetasizer Nano (Nano Series ZS90, Malvern, Britain). The surface area, total pore volume, and micropore volume of GFMs were measured using Autosorb-1 (Quantachrome, USA). Cross polarization magic angle spinning ^{13}C NMR spectrum (Karlsruhe, Germany) was used to analyze the carbon structure and carbon containing functional groups of HA.

2.2 Algal growth inhibition and joint toxicity

Chlorella sp., a kind of unicellular green microalgae, was purchased from Wuhan FACHB-collection, Chinese Academy of Sciences. *Chlorella sp.* was cultivated in 1/10 Selenite Enrichment (SE) medium (pH, 7.0) (Table S1) under 24 °C and 14 h/10 h light/dark cycle (light intensity, 4000 lux).[8]

The algal cells (1×10^6 cells/mL) at exponential-phase were exposed to GFMs (GO, rGO, and G), HA/CA, and GFMs in the presence of HA/CA, respectively. The algae cultivated in 1/10 SE medium was set as the control group. Each treatment was conducted in three replicates. After 96-h incubation, the number of algal cells was counted by hemocytometer on light microscope (LM, BM1000, JNOEC, China). The concentration of GFMs (40 mg/L) used in this work was based on their 96-h median effective concentrations (EC_{50}s) on *Chlorella sp.* in our previous study,[8] and the concentration of HA and CA (20 mg/L) was based on the contents of dissolved organic carbon (1-20 mg/L) in surface water.[25]

We further investigated the joint toxicity effect between GFMs and HA because HA (20 mg/L) alone could also inhibit algal growth. Additive Index (*AI*) method, a traditional method of evaluating joint toxicity in mixture system was employed.[26] Briefly, algal cells were co-exposed to a series of test concentrations of GFMs and HA at a fixed concentration ratio (GFMs: HA, 2:1) for 96 h. This concentration ratio was selected based on the concentrations used in the growth inhibition assay (GFMs, 40 mg/L; HA, 20 mg/L).[27] Then the concentration-response relationship between GFMs-HA mixture and algal cells as well as the EC_{50}s of GFMs and HA in mixture were obtained through microscopical counting. The joint

toxicity could be calculated by

$$S = \frac{GFMm}{GFMi} + \frac{HAm}{HAi} \quad (1)$$

$$AI = (-1) \times S + 1 \ (S \geq 1.0) \text{ or } AI = \frac{1}{S} - 1 \ (S < 1.0) \quad (2)$$

where *GFMi* or *HAi* is EC_{50} value of GFM or HA individually; *GFMm* or *HAm* is the EC_{50} value of GFMs or HA in mixture; *S* is the sum of biological activity; and *AI* is defined as Additive Index. "*AI*=0" indicates that the joint toxicity of materials is simply additive; "*AI*>0" indicates the synergistic effect between two materials; "*AI*<0" indicates the antagonistic effect between two materials. The absolute value of *AI* reflects the level of synergistic or antagonistic effect.

The algal growth inhibition by GFMs in two fresh natural water samples were further investigated. The water samples were collected from Zhangcun river in Qindao (36°10'6" N, 120°30'29" E) and the campus lake of Ocean University of China (36°9'31" N, 120°29'45" E), respectively. Selected properties (pH, conductivity, salinity, and total organic carbon (TOC) content) of these two water samples were examined and listed in Table S2. After filtration through 0.45-μm filter (JIN TENG, China), the water samples were mixed with activated carbon (50 g/L) and shaken (150 rpm) for 12 h. Then the water sample was filtered by 0.22-μm filter (JIN TENG, China). The procedure was repeated twice to insure the sufficient remove of TOC and the TOC-removed natural water sample was obtained.[28] The algae cells were exposed to 40 mg/L GFMs (GO, rGO, and G) in original natural water and TOC-removed water samples for 96 h, respectively, and the growth inhibition was measured by microscopical counting.

2.3 Membrane damage and oxidative stress

Membrane damage of algal cells was assessed by confocal laser scanning microscope (CLSM, Nikon A1+, Japan). The algal cells were exposed to GFMs (GO, rGO, G), HA, and GFM-HA, respectively. The 96-h exposed cells (5×10^6 cells/mL) were stained by SYTO Green (10 μM, Ex/Em 500/530 nm) and propidium iodide (PI, 25 mg/L, Ex/Em 535/615 nm), washed three times with PBS (pH 7.2, 0.1 M), and then detected by CLSM. The fluorescent dye SYTO Green could label all algal cells, while PI could specifically label the membrane-damaged cells during exposure. For each treatment, the percentage of membrane-damaged cells was calculated from the proportion of PI-dyed cells in all cells (SYTO Green-dyed cells) in 8-12 CLSM images.

The generation of ROS in algal cells was determined by 2', 7'-dichlorodihydrofluo-rescein diacetate (DCFH-DA). After exposure to HA (20 mg/L), GFMs (40 mg/L), or GFMs-HA (GFMs, 40 mg/L; HA, 20 mg/L) for 96 h, the algal cells were obtained and dyed with DCFH-DA, and the level of intracellular ROS was detected by fluorescence spectroscopy (Hitachi F4600, Japan) with the excitation wavelength at 488 nm and emission wavelength at 525 nm. Lipid peroxidation level of algal cells was assessed by malondialdehyde (MDA) content using a microplate reader (Thermo, USA) at 532 nm.

2.4 Heteroaggregation and co-sedimentation of GFMs with algal cells in the absence and presence of HA

To determine the effect of HA on the heteroaggregation and co-sedimentation of GFMs with algal cells, a sedimentation experiment was employed in the presence or absence of

HA.[14] Briefly, GFMs suspensions (40 mg/L) were prepared with the assistance of sonication (500 W, 30 min), and then mixed with algae suspension (1×10^6 cells/mL) in the absence or presence of HA (20 mg/L). The turbidity of the suspensions was then continuously examined at 600 nm for 120 min using a UV-Vis spectrophotometer (PerkinElmer, Lambda35, USA). The optical density was calculated by

$$OD_t = A_t/A_0 \quad (3)$$

where OD_t is the optical density at time t (min), A_t is the absorbance of mixed system at time t, and A_0 is the initial absorbance of the mixed suspension.

The theoretically additive settling curves were calculated, and then compared with actually measured ones. The additive settling curves are shown by "+" (e.g., "Alga+GO", and "Alga-GO+HA"), which could be obtained by

$$OD_i = (A_{t1} + A_{t2})/(A_{01} + A_{02}) \quad (4)$$

where OD_i is the theoretically additive optical density, A_{t1} and A_{01} are the absorbance at time t and initial absorbance of one suspension, while A_{t2} and A_{02} are the absorbance at time t and initial absorbance of the other suspension, respectively.

The settling curves were also fitted by an exponential model, that is,

$$y = OD_{plateau} + OD_{reduced}exp\,(-vt) \quad (5)$$

where $OD_{plateau}$ is the optical density at the plateau of the settling curve, $OD_{reduced}$ is the reduced optical density from the initial time to the plateau, v (min^{-1}) is the sedimentation rate, t (min) is the sedimentation time.

2.5 Adsorption of HA on GFMs

The adsorption experiments were conducted using a batch equilibration technique in 15-mL vials at 25 °C. Briefly, GFMs (200 mg/L) and HA solutions (5-100 mg/L) prepared in algal medium were added into vials, and the solution pHs were adjusted to 7.0. Then, the vials were shaken at 150 rpm for 96 h to reach equilibrium. After centrifugation (3000 rpm, 30 min), the equilibrium concentrations of HA in the supernatants were determined at 254 nm by a UV–Vis spectrometer. The HA adsorption experiments were run in triplicate. The Freundlich and Langmuir model were used to fit the adsorption isotherms, and the detailed information was described in the Supporting Information (Experimental S1).

In addition, zeta potential and hydrodynamic diameter of GFMs in the absence or presence of HA in algal medium were determined by Zetasizer Nano (Nano Series ZS90, Malvern, Britain). GFMs before and after HA adsorption were further characterized using scanning electron microscope (SEM, HITACHI S-4800, Japan) and Fourier transform infrared spectroscopy (FTIR, Tensor 27, Bruker Optics, Germany). The morphologies of algal cells after exposure to GFMs in the presence of HA were also observed by SEM.

2.6 Nutrient depletion and shading effect induced by GFMs and HA on algal growth

Nutrient-depletion experiment was designed to identify the adsorption of nutrient elements by GFMs (with and without HA) on algal growth. Briefly, GFMs (40 mg/L), or GFMs in the presence of HA (GFMs, 40 mg/L; HA, 20 mg/L) were added into algal medium in glass containers. After shaken for 96 h, the suspensions were centrifugated (1000 g; 20 min), and filtered with 0.22-μm membrane (JIN TENG, China) to remove GFMs. The obtained supernatants were used for algal growth test. The nutrient adsorption experiments were run in

triplicate. For comparison, a full medium without the removal of nutrient elements was used for algal culturing. After 96-h cultivation, the number of algal cells was determined by hemocytometer counting. In addition, the concentrations of macroelements (Ca, Mg, N, and P) in the supernatant were quantified. The contents of Ca and Mg in the supernatants were determined by inductively coupled plasma mass spectrometry (ICP-MS, NexION 350X, USA). N and P were examined by UV-Vis spectroscopy using alkaline potassium persulfate digestion-UV spectrophotometric method and ammonium molybdate spectrophotometric method, respectively.[29,30]

The light shading induced by GFMs in the absence or presence of HA on algal growth was investigated following our pervious study.[8] Briefly, 250 mL conical flasks with algal cells in algal medium were set in 1-L beakers, which contained HA solution (20 mg/L), GFMs suspension (40 mg/L), or GFMs-HA mixed suspension (GFMs, 40 mg/L; HA, 20 mg/L). The conical flask and the beaker were at the same liquid level. After 96-h cultivation, the number of algal cells in each treatment group was determined by hemocytometer counting.

2.7 Statistical analysis

Statistical analysis of the data was performed using SPSS 22.0 by one-way ANOVA with LSD or T test after the verification of normality and homoscedasticity assumption. All the experiments were run at least in triplicate, and significant difference was analyzed at a "$p < 0.05$" level.

3 Results and discussion

3.1 GFMs and HA characterization

TEM images showed that all the three GFMs had layered structures (Fig. S1). The sheets of GO and G were smooth while rGO showed irregular-folding morphologies due to hydrazine hydrate reduction (Fig. S1). The oxygen contents of GO, rGO and G were 53.5%, 20.8%, and 2.6%, respectively, which reflected the different oxidation degrees of the three types of GFMs (Fig. 1A, 1B, 1C). In addition, the sulfur content of GO was relatively high (2.1%) due to the usage of sulfuric acid during the oxidation process. rGO had the highest nitrogen content among the three GFMs, which was derived from the reductive agent (hydrazine hydrate) during reduction process. Raman spectra showed prominent *G* and *D* peaks of GFMs around 1600 cm^{-1} and 1350 cm^{-1}, which indicated the sp^2 and sp^3 hybrid carbon atoms structure of GFMs, respectively (Fig. 1D).[31] G also had *G'* peak (2764 cm^{-1}) and the intensity ratio of *G*/*G'* peaks (approximately 2.72:1) showed the multi-layered G.[31] The ratio of *D*/*G* peak intensities (I_D/I_G) followed the order: G < GO < rGO, demonstrating that rGO had the most abundant defects in the layered structure among the three GFMs.[32] All the three GFMs were negatively charged in ultrapure water and GO had the strongest electronegativity because of the most content of O-containing functional groups (Fig. 1E). The hydrodynamic diameters of GO, rGO and G in ultrapure water were 441, 998, and 1161 nm, respectively.

The contents of carbon, oxygen and hydrogen within the organic component of HA were 54.1%, 38.9% and 5.0%, respectively (Fig. S2). ^{13}C NMR was used to further analyze the types of carbon composition in HA (Fig. S3). Aromatic carbon, including aryl and O-aryl carbon, accounted for 44.8% among all carbon atoms and the aromaticity reached 47.9%.

Also, HA had a total polar carbon of 19.3%, suggesting abundant functional groups on the surface of HA, such as -C=O, -COOH, -OCH_3 and O-containing aromatic hydrocarbons.[33]

3.2 Joint toxicity of GFMs and HA on algal growth

After 96-h exposure, it was shown that all the three GFMs (40 mg/L) could highly inhibit the growth of algae, with the inhibition rates of 31.9%, 42.9%, and 29.2% for GO, rGO, and G, respectively (Fig. 2A). HA (20 mg/L) also exhibited toxicity to algal cells (growth inhibition, 9.9%). In the presence of HA, the 96-h growth inhibition rates of GO and rGO were significantly decreased by 57.4% and 82.2% as compared to GO or rGO alone ($p < 0.05$). For G, there was no significant difference between the treatments with and without HA. We could not evaluate the joint toxicity (synergetic, additive or antagonistic effects) between GFMs and HA by simply adding up the inhibition rates. Therefore, the *AI* method was employed here for the joint toxicity investigation. The *AI* values between HA and each GFM were calculated based on the concentration-dependent algal growth of GFM and HA (Table S3), and shown in Fig. 2B. GO-HA, rGO-HA, and G-HA had the *AI* values of -5.25, -6.56 and -0.76, clearly suggesting the antagonistic effect between GFMs and HA. For GO, the observed toxicity mitigation in the presence of HA was in good agreement with previous studies on zebrafish embryo, *Scenedesmus obliquus*, and *Escherichia coli*.[16,34,35] For the three types of GFMs, antagonistic effects in the presence of HA followed the order: rGO > GO > G. Zhang et al. also found that HA lowered the toxicity of GFMs to another algal species (*Scenedesmus obliquus*).[17] On the contrary, HA enhanced the accumulation of graphene in zebrafish by 2.5-16 times.[21] The surface coating (e.g., CA) could also increase the accumulation of Ag NPs

in zebrafish.[36] Therefore, the joint toxicity (synergetic or antagonistic effects) between NOM and nanomaterials should also be organic species-dependent, which needs further investigation. In addition, it seems that the toxicity reduction is not simply related to the oxygen contents or oxidation degrees of GFMs in the present work. The mechanisms for the observed toxicity mitigation was investigated in the following sections.

It was reported that low-molecular weight organic matter as SDBS and TX100 could increase the toxicity of multiwalled CNTs while high-molecular weight HA alleviated the toxicity to algae (*Chlorella sp.*).[14] Therefore, CA, another representative NOM with low-molecular weight was used to verify the antagonistic effect between NOM and GFMs. Similarly, CA significantly mitigated the toxicity of all the three GFMs to algal cells (Fig. S4). To better understand GFMs toxicity in natural environments, two natural water samples were obtained from Zhangcun River and campus lake, with the TOC content at 21.1 and 90.7 mg C/L, respectively (Table S2). The toxicity of GFMs in original and TOC-removed natural waters (3.2 and 3.7 mg C/L for the two natural waters after TOC removal) was investigated. It was shown that the toxicity of all the three GFMs to algae in the original natural waters was much lower than that in the TOC-removed natural waters for both water samples (Fig. S5A, S5B). Toxicity reduction was much more obvious in the natural water from campus lake with higher TOC content in comparison with that from Zhangcun River, showing that TOC in natural water mitigated the toxicity of GFMs to algae. This finding was in good agreement with the toxicity reduction in the presence of HA and CA (Fig. 2, S4). Hence, it is likely that both high- and low-molecular weight NOM as well as complicated NOMs in natural water

could mitigate the toxicity of GFMs on algal growth. HA, a ubiquitous form of NOM, was chosen as the model NOM in the following mechanistic investigation on NOM-induced toxicity mitigation.

3.3 HA alleviated GFM-induced membrane damage and oxidative stress

Membrane damage is an important indicator for GFM-induced toxicity,[6] which was detected by CLSM after dying with SYTO Green and PI probes (Fig. S6). HA alone did not significantly induce membrane damage of algal cells. GO, rGO and G exhibited 21.0%, 33.8%, and 28.5% of membrane damage, respectively. In the presence of HA, membrane damage was mitigated for all the three GFMs (Fig. S6, 3A). rGO showed the highest mitigation (29.3%) in the presence of HA in comparison with GO (22.9%) and G (28.4%). This was in good agreement with the growth inhibition investigation, in which rGO had the strongest toxicity mitigation by HA (Fig. 2), demonstrating that HA mitigated GFM-induced toxicity through decreasing membrane damage.

Oxidative stress, an important mechanism for membrane damage, was investigated in the absence and presence of HA. Intracellular ROS levels were triggered after 96-h exposure to the three GFMs (Fig. 3B), which may be induced by the sp^2 hybridized electron structure, which would increase the oxidation of intracellular glutathione or directly accelerate the electron transfer between the edges of GFMs and biological membrane.[1] rGO induced the strongest oxidative stress to algal cells, which may be attributed to the highest defect level (highest I_D/I_G value in Fig. 1D) in sp^2 hybridized electron structure and the highest conductivity among the three GFMs.[37] It should be noted that intracellular ROS levels of algal

cells were significantly decreased in the presence of HA, suggesting that HA could reduce GFMs-induced oxidative stress in algal cells. It was shown that MDA contents of algal membrane after GFMs exposure followed an order of rGO > GO > G (Fig. 3C), which was consistent with the intracellular ROS generation. Similarly, HA significantly decreased the contents of MDA in algal membrane, showing that HA mitigated GFMs-induced membrane permeability through regulating intracellular ROS generation.

3.4 Heteroaggregation of GFMs and algal cells in the presence of HA.

During GFMs exposure, the heteroaggregation of GFMs with algae was observed using LM. Algal cells in the medium were uniformly distributed on hemocytometer, and HA did not change the distribution of algal cells (Fig. S7). During GFMs exposure, the heteroaggregates of algal cells and rGO/G were observed. In the heteroaggregates, the accumulated algal cells could directly contact with rGO/G and suffer stronger membrane damage than the free algal cells. In addition, algae-rGO/G heteroaggregation may lower the bioavailability of light and nutrients, thus causing growth inhibition of the accumulated algal cells. In the presence of HA, the heteroaggregates of algae-rGO/G were still observed, but the aggregates sizes were obviously decreased (Fig. S7), indicating the decrease in direct contact between algal cells and rGO/G. For GO, it was difficult to be observed on the hemocytometer through LM because of the high transparency of GO sheets. We thus further observed the algal cells exposed to GO and GO-HA through the light field of the confocal microscope (Fig. S8). GO did not heteroaggregate with algal cells, and could not influence algal distribution, indicating that the

direct contact between algal cells and GO was relatively weak. After adding HA, the distribution of algae was not changed either.

Considering the change of algae-GFM heteroaggregation in the presence of HA (Fig. S7), it was speculated that HA may influence the dispersion stability of GFMs and algal cells in algal medium. Co-sedimentation between algal cells and GFMs was examined in the absence or presence of HA, and the model-fitted parameters of settling curves were acquired (Table S4). As a type of plankton, *Chlorella sp.* cells suspended well in the medium. The dispersion stability of GO was much higher than rGO and G (Fig. S9, Table S4) due to abundant O-containing groups and the highest electronegativity (Fig. 1E). In the GFM-algae binary system, co-sedimentation was not observed for GO based on the overlapped settling curves of theoretically additive A/A_0 values and measured values. Co-sedimentation occurred between algal cells and rGO/G, probably due to strong heteroaggregation, which was reflected by the higher theoretically additive A/A_0 values relative to the measured values.[14] The co-sedimentation process could be harmful to the growth of algae that were captured by rGO/G due to the isolation from normal living environment and adaptive nutrients. In algae-GFM-HA system, HA had no effect on the heteroaggregation between algal cells and GO (Fig. 4, Table S4), which was mostly due to the original stability of GO and algal cells. However, HA clearly improved the suspension stability of algae-rGO/G. Meanwhile, the measured settling curves were higher than the theoretically additive curves of algae-GFM-HA for both rGO and G, suggesting that HA decreased the heteroaggregation between rGO/G and

algal cells, which was in good agreement with the changes of heteroaggregates as acquired from LM images (Fig. S7). As a result, the direct contact of algae with rGO/G was weakened.

3.5 Adsorption of HA on GFMs

To understand the interaction of HA with GFMs, HA adsorption on the three types of GFMs was investigated, and the adsorption isotherms were shown in Fig. 5A. The isotherms were fitted by Freundlich and Langmuir models, and Freundlich model had better fitting results for the isotherms of rGO and G as indicated by higher "R_{adj}^2", while Langmuir model had better fitting results for GO (Table S5). Clearly, all the three GFMs could adsorb HA molecules, and the adsorption capacity followed the order: GO > G > rGO. We further determined the specific surface area, total pore volume and DR micropore volume of GFMs (Table S6). GO with the lowest surface area and pore volume showed the highest adsorption capacity among three GFMs, indicating that surface occupation and pore filling did not play an important role in HA adsorption. In addition, GO had the highest hydrophilicity and electronegativity (Fig. 1E) among the three GFMs. Hydrophobic and electrostatic attractions were therefore not the dominant mechanism for HA adsorption. Moreover, GO had much lower benzene ring-based structures than rGO and G, and π-π interaction should not be a main reason for the highest HA adsorption. Considering the abundant O-containing groups and H content for both GO (Fig. 1A) and HA (Fig. S2, S3), hydrogen bonding could be the dominant interaction for GO-HA interaction.[38]

We further characterized the interaction between GO and HA using FTIR (Fig. S10). GO exhibited typical O-containing functional groups, such as C=O, epoxy C-O, and alkoxy C-O,

and there was typical C=N group on HA. The C=N group was not observed in GO but present in GO-HA after 96-h adsorption, confirming the adsorption of HA on GO. After HA adsorption, zeta potentials were more negative for all the three GFMs (Fig. 5B) because of abundant negatively charged O-containing groups on HA molecules (-37.9±0.3 mV in algal medium). The hydrodynamic diameters of GFMs (especially for rGO and G) in the presence of HA were correspondingly decreased relative to bare GFMs (Fig. S11) due to enhanced electrostatic repulsion. Meanwhile, algal cell surface was negatively charged (-20.2 mV),[8] and the electrostatic repulsion between algal cells and HA-coated GFMs should be stronger than bare GFMs. This could explain the finding on the decreased heteroaggregation between rGO/G and algal cells in the presence of HA (Fig. 4, S7). Ha et al. reported that HA augmented the surface negative charges of fullerene after HA adsorption, thus significantly alleviating the accumulation of fullerene in Caco-2 cells.[39] A similar finding was gained by Kang et al., which reported that elevated NOM concentration reduced the attachment of bacteria on single-walled CNTs by 50%.[40]

HA adsorption on GFMs was further observed using SEM. The surfaces of GFMs were occupied with HA molecules (indicated with yellow arrows) after adsorption in comparison with pristine GFMs (Fig. 5C, 5D, 5E, Fig. S12). In GFM-HA-algae system, the HA-coated GFMs were still observed, and most of algae did not aggregate with HA-coated GFMs. Steric hindrance between GFMs and algae would exist due to the existence of HA molecules on GFMs, which could be another reason to prevent the direct contact of GFMs with algal cells in addition to electrostatic repulsion.[41,42]

3.6 Nutrient depletion and shading effect of GFMs as affected by HA

GFMs could adsorb nutrients and cause the depletion of bioavailable nutrients for algal growth.[8] In the present work, GFMs were incubated in algal medium (both with and without HA) for 96 h to adsorb nutrients, and the GFMs-removed supernatants were used to cultivate algal cells. In the absence of HA, all the three GFMs-removed supernatants (containing the remained nutrients) significantly inhibited the growth of algal cells (Fig. 6A). In the presence of HA, the growth of algae cultured in the GO-removed supernatants (containing the remained nutrients and HA) was significantly increased by 9.9% ($p < 0.05$), demonstrating that HA reduced the depletion of nutrient elements caused by GO. It should be noted that this observed growth increase should be more obvious because HA in the supernatants was toxic to algae as indicated in Fig. 2A. However, HA did not change the nutrient-depletion effect of rGO and G.

It was reported that Ca, Mg, N, and P were the main nutrients that were depleted by GFMs.[8] We thus further investigated the removal of these nutrients in the presence of HA. After adsorption by GFMs alone (in the absence of HA), the contents of Ca, Mg, and P significantly decreased compared with their original contents in the algal medium (Fig. 6B, 6C, 6D). In the presence of HA, the contents of Ca increased by 72.6%, 80.9%, and 12.8% in the supernatants after the removal of GO, rGO and G, respectively. Mg contents in the presence of HA increased by 46.2% and 21.1% for GO and rGO in comparison with GO/rGO alone (in the absence of HA) while HA did not change the content of Mg in medium for G. GO had the highest increase in Mg content in the supernatants in the presence of HA, which was probably because of strongest competition between Mg and HA on GO surface relative to

other GFMs. For P, HA increased its content in the supernatants by 7.9%, 5.0%, and 9.2% when compared with the treatments of GO, rGO, or G alone (Fig. 6D). For N content, there was no significant difference between GFM and GFM-HA treatments for all the three GFMs (Fig. S13), suggesting that N had no relationship with the HA-induced mitigation of nutrient depletion. Because HA mitigated nutrient depletion-induced growth inhibition caused by GO but did not influence nutrient depletion from rGO and G (Fig. 6A), the increase of Mg content rather than other nutrients (e.g., Ca, N, P) could be a critical reason for the observed reduction in GO-induced nutrient depletion. Mg^{2+} is essential for photosynthesis as well as enzymatic activities.[8] Thus, the increase in Mg content after the addition of HA may have reduced the inhibition of photosynthesis and algal growth through the alleviation of Mg-depletion.

Light utilization is important for algal growth. HA or GFMs alone did not induce shading effect on algal growth, probably because of insignificant blocking in light transmittance (Fig. S14, S15). However, HA enhanced shading effect from GO. This was probably because of the darker color of suspension, which further decreased light transmittance in algal medium (Fig. S14, S15). For rGO and G, HA had no influence on their shading effect, which can be explained by the settling of rGO and G in the presence of HA in comparison with HA or GO alone (Fig. S15). All these findings suggested that the change in shading effect was not responsible for the alleviation in GFMs toxicity caused by HA.

4 Conclusions

NOM is ubiquitously existing in natural aquatic environments, and inevitably participates in the interaction of GFMs with aquatic organisms. In the present work, it was observed that

GFMs-induced toxicity to algae was highly mitigated in the presence of NOM for all the three types of GFMs. The joint toxicity investigation showed the antagonistic effect between GFMs and HA, which followed the order of rGO > GO > G. The mitigation of algal membrane damage was confirmed as a main mechanism for the observed decrease in GFMs-induced toxicity in the presence of HA. Further investigation showed that HA could alleviate GFMs-induced membrane damage through decreasing intracellular ROS and lipid peroxidation. In addition, the decrease in direct contact between GFMs and algae by HA could also reduce membrane damage, and the direct contact was lowered by weakened GFMs-algae heteroaggregation (for rGO and G) and enhanced steric hindrance (for GO, rGO, and G). Moreover, the nutrient depletion caused by GO was significantly corrected by HA, and could contribute to the mitigation of GO-induced toxicity to algae. Our study suggests that the toxicity of GFMs could be overestimated based on current laboratory toxicological investigations due to the presence of NOM in natural aquatic environments. To assess environmental risk and fate of GFMs, the effect of NOM and other environmentally relevant conditions should be taken into full consideration.

Supplementary information

Fourteen figures and six tables. This material is available free of charge via the Internet at http://pubs.rsc.org/.

Conflicts of interest

There are no conflicts to declare.

Acknowledgement

This research was supported by National Natural Science Foundation of China (41822705, 41530642, 41573092, 41629101), the Youth Talent Support Program of the Laboratory for Marine Ecology and Environmental Science, Pilot National Laboratory for Marine Science and Technology (Qingdao) (LMEES-YTSP-2018-02-09), Natural Science Foundation of Shandong Province (JQ201805), and USDA-NIFA Hatch program (MAS 00475).

References

1. J. Zhao, Z. Wang, J. C. White and B. Xing, Graphene in the aquatic environment: adsorption, dispersion, toxicity and transformation, *Environ. Sci. Technol.*, 2014, **48**, 9995-10009.
2. K. S. Novoselov, V. I. Fal, L. Colombo, P. R. Gellert, M. G. Schwab and K. Kim, A roadmap for graphene, *Nature*, 2012, **490**, 192-200.
3. A. K. Geim and K. S. Novoselov, The rise of graphene, *Nat. Mater.*, 2007, **6**, 183-191.
4. D. G. Goodwin Jr, A. S. Adeleye, L. Sung, K. T. Ho, R. M. Burgess and E. J. Petersen, Detection and quantification of graphene-family nanomaterials in the environment, *Environ. Sci. Technol.*, 2018, **52**, 4491-4513.
5. R. Li, N. D. Mansukhani, L. M. Guiney, Z. Ji, Y. Zhao, C. H. Chang, C. T. French, J. F. Miller, M. C. Hersam, A. E. Nel and T. Xia, Identification and optimization of carbon radicals on hydrated graphene oxide for ubiquitous antibacterial coatings, *ACS Nano*, 2016, **10**, 10966-10980.
6. V. T. Pham, V. K. Truong, M. D. J. Quinn, S. M. Notley, Y. Guo, V. A. Baulin, M. A. Kobaisi, R. J. Crawford and E. P. Ivanova, Graphene induces formation of pores that kill spherical and rod-shaped bacteria, *ACS Nano*, 2015, **9**, 8458-8467.

7. F. Perreault, A. F. De Faria, S. Nejati and M. Elimelech, Antimicrobial properties of graphene oxide nanosheets: why size matters, *ACS Nano*, 2015, **9**, 7226-7236.

8. J. Zhao, X. Cao, Z. Wang, Y. Dai and B. Xing, Mechanistic understanding toward the toxicity of graphene-family materials to freshwater algae, *Water Res.*, 2017, **111**, 18-27.

9. C. Pretti, M. Oliva, R. D. Pietro, G. Monni, G. Cevasco, F. Chiellini, C. Pomelli and C. Chiappe, Ecotoxicity of pristine graphene to marine organisms, *Ecotoxicol. Environ. Saf.*, 2014, **10**, 138-145.

10. A. L. Fernandes, M. E. Josende, J. P. Nascimento, A. P. Santos, S. K. Sahoo, F. M. R. da Silva, L. A. Romano, C. A. Furtado, W. Wasielesky, J. M. Monserrat and J. Ventura-Lima, Exposure to few-layer graphene through diet induces oxidative stress and histological changes in the marine shrimp *Litopenaeus vannamei*, *Toxicol. Res.*, 2017, **6**, 205-214.

11. Y. Kim, J. Jeong, J. Yang, S. Joo, J. Hong and J. Choi, Graphene oxide nano-bio interaction induces inhibition of spermatogenesis and disturbance of fatty acid metabolism in the nematode *Caenorhabditis elegans*, *Toxicology*, 2018, **410**, 83-95.

12. A. L. Fernandes, J. P. Nascimento, A. P. Santos, C. A. Furtado, L. A. Romano, C. E. Rosa, J. M. Monserrat and J. Ventura-Lima, Assessment of the effects of graphene exposure in *Danio rerio*: a molecular, biochemical and histological approach to investigating mechanisms of toxicity, *Chemosphere***,** 2018, **210**, 458-466.

13. J. Chen, G. Zhou, L. Chen, Y. Wang, X. Wang and S. Zeng, Interaction of graphene and its oxide with lipid membrane: a molecular dynamics simulation study, *J. Phys. Chem. C*, 2016, **120**, 6225-6231.

14. L. Zhang, C. Lei, J. Chen, K. Yang, L. Zhu and D. Lin, Effect of natural and synthetic surface coatings on the toxicity of multiwalled carbon nanotubes toward green algae, *Carbon*, 2015, **83**, 198-207.

15. J. Zhao, Y. Dai, Z. Wang, W. Ren, Y. Wei, X. Cao and B. Xing, Toxicity of GO to freshwater algae in the presence of Al_2O_3 particles with different morphologies: importance of heteroaggregation, *Environ. Sci. Technol.*, 2018, **52**, 13448-13456.

16. Y. Zhang, T. Meng, L. Shi, X. Guo, X. Si, R. Yang and X. Quan, The effects of humic acid on the toxicity of graphene oxide to *Scenedesmus obliquus* and *Daphnia magna*, *Sci. Total Environ.*, 2019, **649**, 163-171.

17. Y. Zhang, T. Meng, X. Guo, R. Yang, X. Si and J. Zhou, Humic acid alleviates the ecotoxicity of graphene-family materials on the freshwater microalgae *Scenedesmus obliquus*, *Chemosphere*, 2018, **197**, 749-758.

18. R. Zouzelka, P. Cihakova, J. R. Ambrozova and J. Rathousky, Combined biocidal action of silver nanoparticles and ions against Chlorococcales (*Scenedesmus quadricauda*, *Chlorella vulgaris*) and filamentous algae (*Klebsormidium sp.*), *Environ. Sci. Pollut. Res.*, 2016, **23**, 8317-8326.

19. R. Roy, A. Parashar, M. Bhuvaneshwari, N. Chandrasekaran and A. Mukherjee, Differential effects of P25 TiO_2 nanoparticles on freshwater green microalgae: *Chlorella* and *Scenedesmus* species, *Aquat. Toxicol.*, 2016, **176**, 161-171.

20. H. Pendashte, F. Shariati, A. Keshavarz and Z. Ramzanpour, Toxicity of zinc oxide nanoparticles to *Chlorella vulgaris* and *Scenedesmus dimorphus* algae species, *World J. Fish Mar. Sci.*, 2013, **5**, 563-570.

21. K. Lu, S. Dong, E. J. Petersen, J. Niu, X. Chang, P. Wang, S. Lin, S. Gao and L. Mao, Biological uptake, distribution, and depuration of radio-labeled graphene in adult zebrafish: effects of graphene size and natural organic matter, *ACS Nano*, 2017, **11**, 2872−2885.

22. I. Chowdhury, N. D. Mansukhani, L. M. Guiney, M. C. Hersam and D. Bouchard, Aggregation and stability of reduced graphene oxide: complex roles of divalent cations, pH, and natural organic matter, *Environ. Sci. Technol.*, 2015, **49**, 10886-10893.

23. B. Smith, J. Yang, J. L. Bitter, W. P. Ball and D. H. Fairbrother, Influence of surface oxygen on the interactions of carbon nanotubes with natural organic matter, *Environ. Sci. Technol.*, 2012, **46**, 12839-12847.

24. D. C. Marcano, D. V. Kosynkin, J. M. Berlin, A. Sinitskii, Z. Sun, A. Slesarev, L. B. Alemany, W. Lu and J. M. Tour, Improved synthesis of graphene oxide, *ACS Nano*, 2010, **4**, 4806-4814.

25. F. F. Liu, J. Zhao, S. Wang and B. Xing, Adsorption of sulfonamides on reduced graphene oxides as affected by pH and dissolved organic matter, *Environ. Pollut.*, 2016, **210**, 85-93.

26. L. L. Marking and V. K. Dawson, Method for assessment of toxicity or efficacy of mixtures of chemicals (No. 67), *US Fish and Wildlife Service*, 1975.

27. S. Wu, X. Li, X. Liu, G. Yang, X. An, Q. Wang and Y. Wang, Joint toxic effects of triazophos and imidacloprid on zebrafish (*Danio rerio*), *Environ. Pollut.*, 2018, **235**, 470-481.

28. J. L. Gomez-Eyles, C. Yupanqui, B. Beckingham, G. Riedel, C. Gilmour and U. Ghosh, Evaluation of biochars and activated carbons for in situ remediation of sediments impacted with organics, mercury, and methylmercury, *Environ. Sci. Technol.*, 2013, **47**, 13721-13729.

29. X. Zhang, F. Zhu, L. Chen, Q. Zhao and G. Tao, Removal of ammonia nitrogen from wastewater using an aerobic cathode microbial fuel cell, *Bioresour. Technol.*, 2013, **146**, 161-168.

30. T. Basta, H. Wu, M. K. Morphew, J. Lee, N. Ghosh, J. Lai, J. M. Heumann, K. Wang, Y. C. Lee, D. C. Rees and M. H. Stowell, Self-assembled lipid and membrane protein polyhedral nanoparticles, *Proc. Natl. Acad. Sci. U. S. A.*, 2014, **111**, 670-674.

31. M. S. Dresselhaus, A. Jorio, M. Hofmann, G. Dresselhaus and R. Saito, Perspectives on carbon nanotubes and graphene Raman spectroscopy, *Nano lett.*, 2010, **10**, 751-758.

32. O. Akhavan and E. Ghaderi, Toxicity of graphene and graphene oxide nanowalls against bacteria, *ACS Nano*, 2010, **4**, 5731-5736.

33. K. Sun, J. Jin, M. Kang, Z. Zhang, Z. Pan, Z. Wang, F. Wu and B. Xing, Isolation and characterization of different organic matter fractions from a same soil source and their phenanthrene sorption, *Environ. Sci. Technol.*, 2013, **47**, 5138-5145.

34. Y. Chen, C. Ren, S. Ouyang, X. Hu and Q. Zhou, Mitigation in multiple effects of graphene oxide toxicity in zebrafish embryogenesis driven by humic acid, *Environ. Sci. Technol.*, 2015, **49**, 10147-10154.

35. X. Zhang, M. Sui, X. Yan, T. Huang and Z. Yuan, Mitigation in the toxicity of graphene oxide nanosheets towards *Escherichia coli* in the presence of humic acid, *Environ. Sci.: Processes Impacts*, 2016, **18**, 744-750.

36. H. Liu, X. Wang, Y. Wu, J. Hou, S. Zhang, N. Zhou and X. Wang, Toxicity responses of different organs of zebrafish (*Danio rerio*) to silver nanoparticles with different particle sizes and surface coatings, *Environ. Pollut.*, 2019, **246**, 414-422.

37. L. Tao, M. Qiao, R. Jin, Y. Li, Z. Xiao, Y. Wang, N. Zhang, C. Xie, Q. He, D. Jiang, G. Yu, Y. Li and S. Wang, Bridging the surface charge and catalytic activity of a defective carbon electrocatalyst, *Angew. Chem. Int. Ed.*, 2019, **58**, 1019–1024.

38. T. Hartono, S. Wang, Q. Ma and Z. Zhu, Layer structured graphite oxide as a novel adsorbent for humic acid removal from aqueous solution, *J. Colloid Interface Sci.*, 2009, **333**, 114-119.

39. Y. Ha, X. Wang, H. M. Liljestrand, J. A. Maynard and L. E. Katz, Bioavailability of fullerene under environmentally relevant conditions: effects of humic acid and fetal bovine serum on accumulation in lipid bilayers and cellular uptake, *Environ. Sci. Technol.*, 2016, **50**, 6717-6727.

40. S. Kang, M. S. Mauter and M. Elimelech, Microbial cytotoxicity of carbon-based nanomaterials: implications for river water and wastewater effluent, *Environ. Sci. Technol.*, 2009, **43**, 2648-2653.

41. Q. Li, B. Xie, Y. S. Hwang and Y. Xu, Kinetics of C_{60} fullerene dispersion in water enhanced by natural organic matter and sunlight, *Environ. Sci. Technol.*, 2009, **43**, 3574-3579.

42. Y. Jiang, R. Raliya, P. Liao, P. Biswas and J. D. Fortner, Graphene oxides in water: assessing stability as a function of material and natural organic matter properties, *Environ. Sci.: Nano*, 2017, **4**, 1484-1493.

Figures:

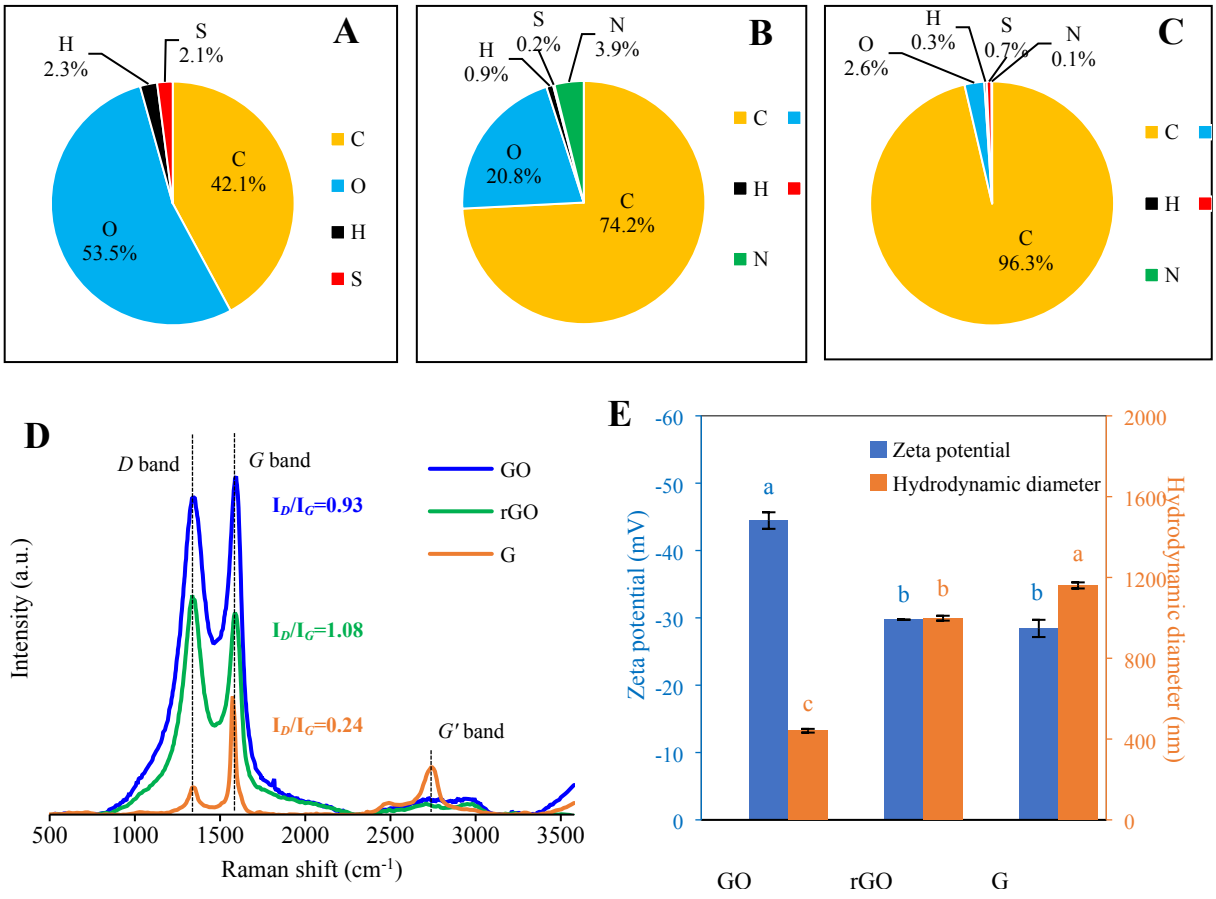

Fig. 1. Physicochemical properties of GFMs. (A), (B), and (C): Elemental compositions of GO, rGO, and G, respectively. (D): Raman spectra of the three GFMs. (E): Zeta potentials and hydrodynamic diameters of GFMs in ultrapure water. In panel E, for each parameter, significant differences among GFMs are marked with different letters (p<0.05, LSD, n=3).

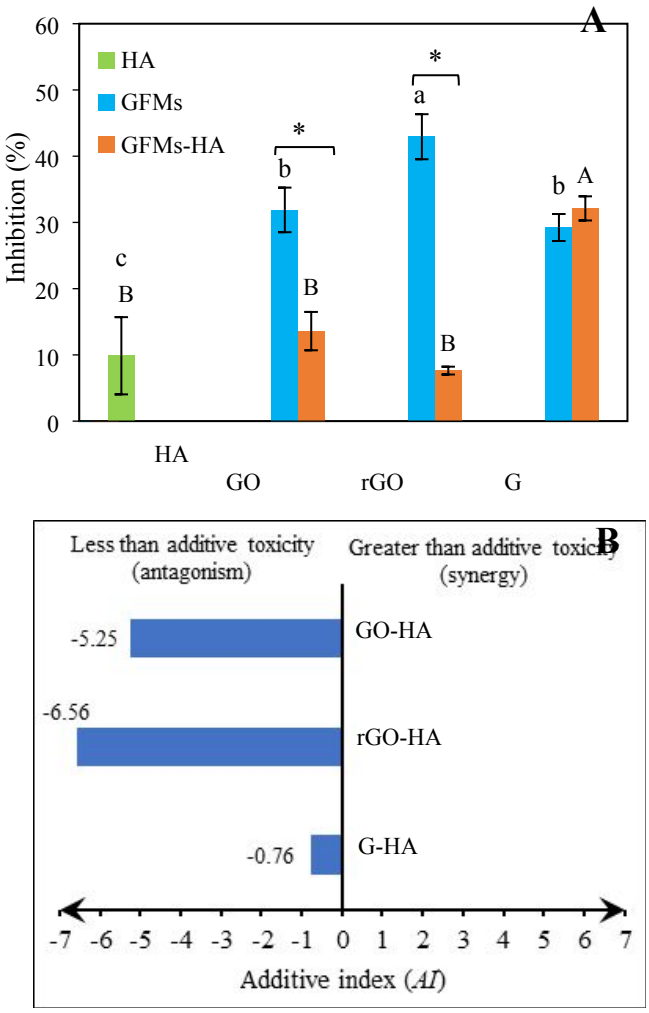

Fig. 2. Effect of HA on the toxicity of GFMs to algae. (A): Inhibition of algal growth by GFMs in the presence of HA. The concentrations of GFMs and HA were 40 and 20 mg/L, respectively. (B): Joint toxicity between HA and GFMs by Additive index (*AI*) analysis. The negative and positive *AI* values in panel B indicate antagonistic effect and synergistic effect, respectively. In panel A, significant differences among HA, GO, rGO, and G treatments are marked with different lowercase letters (p<0.05, LSD, n=3). Significant difference among HA, GO-HA, rGO-HA, and G-HA treatments are marked with different capital letters (p<0.05, LSD, n=3). For a given GFMs, significant difference between GFMs and GFMs-HA is marked with "*" (p<0.05, T test, n=3).

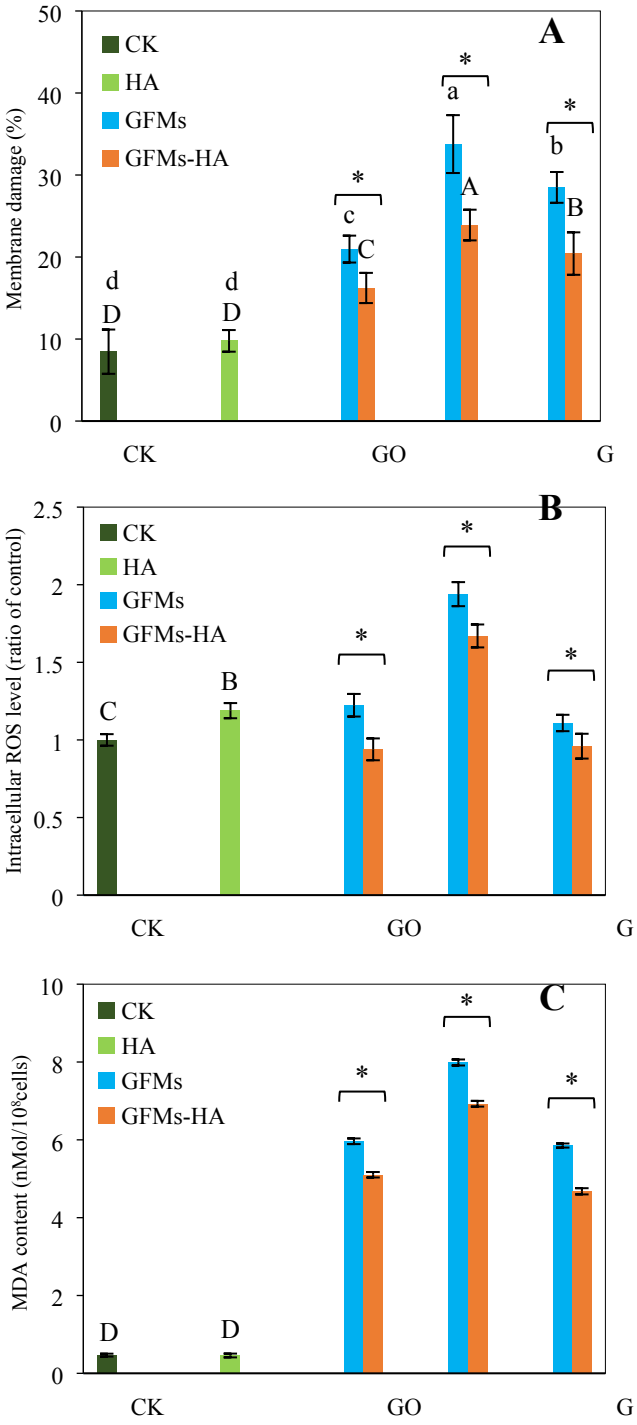

Fig. 3. GFMs-induced membrane damage and oxidative stress of algal cells after exposure to GFMs in the absence or presence of HA. (A): Quantitative data of algal membrane damage results obtained from CLSM analysis. Algal cells were exposed to GFMs (40 mg/L) in the absence and presence of HA (20 mg/L) for 96 h. (B): Intracellular ROS levels of algal cells after exposure to GFMs (40 mg/L) in the absence or presence of HA (20 mg/L) for 96 h. (C):

MDA content in algal cells after exposure to GFMs (40 mg/L) in the absence or presence of HA (20 mg/L) for 96 h. “CK” represents un-exposed algal cells without HA or GFMs exposure. In each panel, significant differences among CK, HA, GO, rGO, and G treatments are marked with different lowercase letters (p<0.05, LSD, n=3). Significant difference among CK, HA, GO-HA, rGO-HA, and G-HA treatments are marked with different capital letters (p<0.05, LSD, n=3). For a given GFMs, significant difference between GFMs and GFMs-HA is marked with “*” (p<0.05, T test, n=3).

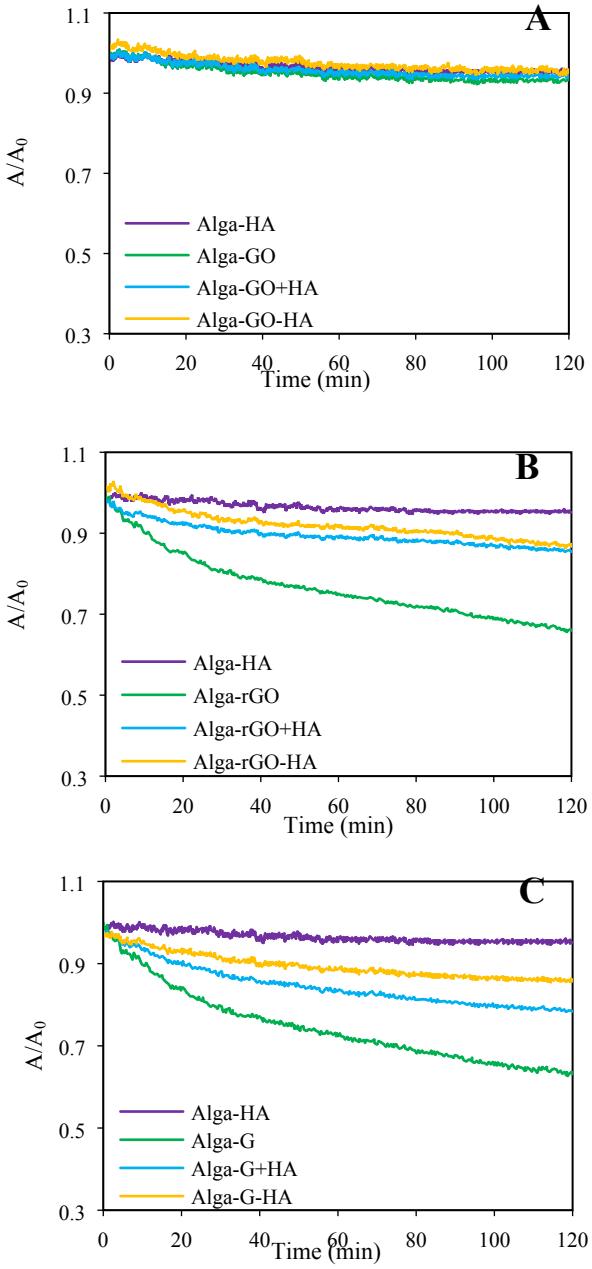

Fig. 4. The settling curves of algal cells and GFMs as affected by HA. (A), (B), and (C): Settling curves of algal cells with GO, rGO, and G, respectively. For each panel, "Alga-GFMs+HA" represents the theoretically additive settling curves of Alga-GFMs and HA, while "Alga-GFMs-HA" represents the actual settling curves of algae, GFMs, and HA. The settling curves were detected for 2 h after the incubation of algal cells with GFMs in the absence or presence of HA in the algal medium.

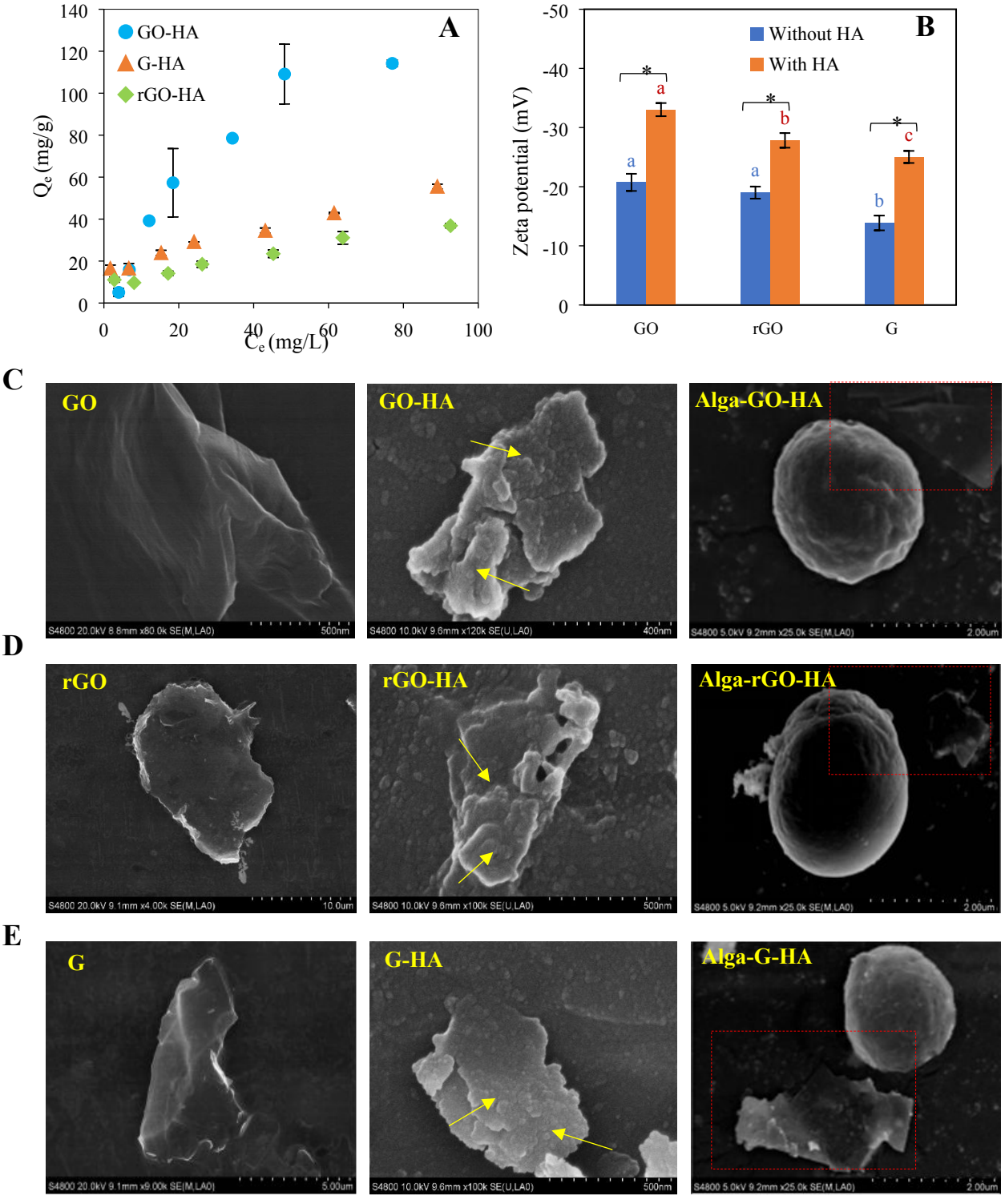

Fig. 5. Adsorption of HA on GFMs. (A): Adsorption isotherms of HA on GFMs in algal medium. (B): Zeta potentials of GFMs in the presence of HA in algal medium (pH, 7; GFMs, 40 mg/L; HA, 20 mg/L). (C), (D) and (E): SEM images of GFMs (GO, rGO, and G) in the

absence of HA, in the presence of HA, and in the presence of HA and algae. Yellow arrows in SEM images indicate the adsorbed HA molecules on GFMs surface and the red frames indicate the reduced contact opportunity between algal cells and GFMs as affected by HA. In panel B, for a given treatment (with or without HA), significant differences among GFMs are marked with different letters (p<0.05, LSD, n=3). For a given GFMs, significant difference between GFMs and GFMs-HA is marked with "*" (p<0.05, T test, n=3).

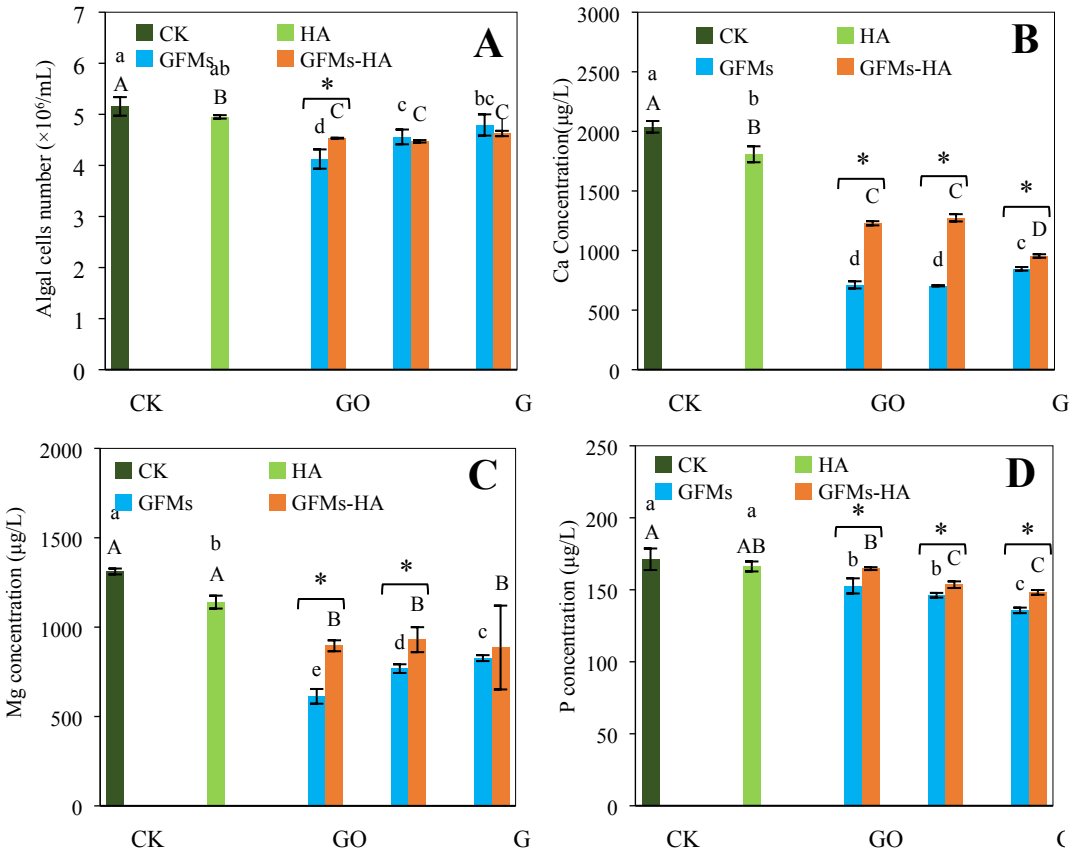

Fig. 6. Effect of HA on the GFMs-induced nutrient depletion and related algal growth. (A): Inhibition of algal growth after exposure to GFMs-removed (40 mg/L) supernatants in the absence and presence of HA (20 mg/L) in medium for 96 h; (B), (C), and (D): Concentrations of Ca, Mg, and P in the supernatants after adsorption, respectively. In panel A, "CK" represents un-exposed algal cells without HA or GFMs exposure. In panel B, C, and D, "CK" represents pristine algal medium. In each panel, significant differences among CK, HA, GO, rGO, and G treatments are marked with different lowercase letters (p<0.05, LSD, n=3). Significant differences among CK, HA, GO-HA, rGO-HA, and G-HA treatments are marked with different capital letters (p<0.05, LSD, n=3). For a given GFMs, significant difference between GFMs and GFMs-HA is marked with "*" (p<0.05, T test, n=3).

Graphic Abstract：

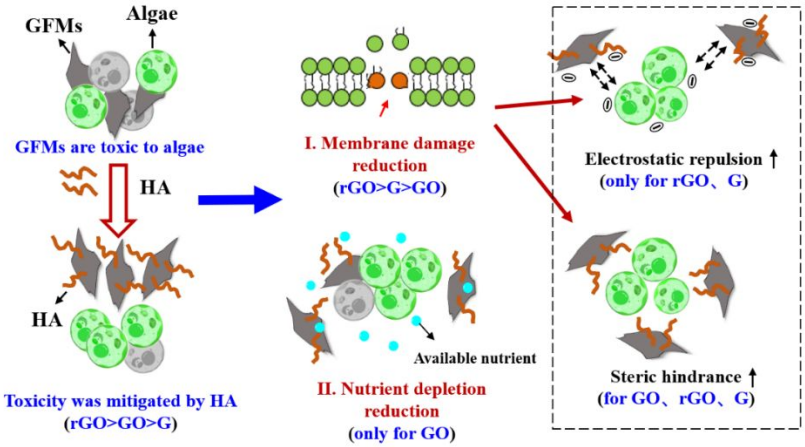

HA alleviated GFMs-induced membrane damage by reducing oxidative stress and heteroaggregation